Aging Cell (2012) **11,** pp520–529 Doi: 10.1111/j.1474-9726.2012.00815.x

An altered redox balance mediates the hypersensitivity of Cockayne syndrome primary fibroblasts to oxidative stress

Barbara Pascucci,[1,2]* Tiziana Lemma,[2]* Egidio Iorio,[3] Sara Giovannini,[2] Bruno Vaz,[4] Ivano Iavarone,[2] Angelo Calcagnile,[2] Laura Narciso,[2] Paolo Degan,[5] Franca Podo,[3] Vera Roginskya,[6,7] Bratislav M. Janjic,[7] Bennett Van Houten,[6,7] Miria Stefanini,[4] Eugenia Dogliotti[2] and Mariarosaria D'Errico[2]

[1]Istituto di Cristallografia, Consiglio Nazionale delle Ricerche, Via Salaria, Km 29,300, 00016 Monterotondo Stazione, Rome, Italy
[2]Department of Environment and Primary Prevention, Istituto Superiore di Sanità, Viale Regina Elena 299, 00161 Rome, Italy
[3]Department of Cell Biology and Neurosciences, Istituto Superiore di Sanità, Viale Regina Elena 299, 00161 Rome, Italy
[4]Istituto di Genetica Molecolare, Consiglio Nazionale delle Ricerche, Via Abbiategrasso 207, 27100 Pavia, Italy
[5]IRCCS Azienda Ospedaliera Universitaria San Martino – IST – Istituto Nazionale per la Ricerca sul Cancro, Largo Rosanna Benzi 10, 16132, Genova, Italy
[6]Department of Pharmacology and Chemical Biology, School of Medicine, University of Pittsburgh, Pittsburgh, PA 15213, USA
[7]Hillman Cancer Center, The University of Pittsburgh Cancer Institute, Pittsburgh, PA 15213, USA

Summary

Cockayne syndrome (CS) is a rare hereditary multisystem disease characterized by neurological and development impairment, and premature aging. Cockayne syndrome cells are hypersensitive to oxidative stress, but the molecular mechanisms involved remain unresolved. Here we provide the first evidence that primary fibroblasts derived from patients with CS-A and CS-B present an altered redox balance with increased steady-state levels of intracellular reactive oxygen species (ROS) and basal and induced DNA oxidative damage, loss of the mitochondrial membrane potential, and a significant decrease in the rate of basal oxidative phosphorylation. The Na/K-ATPase, a relevant target of oxidative stress, is also affected with reduced transcription in CS fibroblasts and normal protein levels restored upon complementation with wild-type genes. High-resolution magnetic resonance spectroscopy revealed a significantly perturbed metabolic profile in CS-A and CS-B primary fibroblasts compared with normal cells in agreement with increased oxidative stress and alterations in cell bioenergetics. The affected processes include oxidative metabolism, glycolysis, choline phospholipid metabolism, and osmoregulation. The alterations in intracellular ROS content, oxidative DNA damage, and metabolic profile were partially rescued by the addition of an antioxidant in the culture medium suggesting that the continuous oxidative stress that characterizes CS cells plays a causative role in the underlying pathophysiology. The changes of oxidative and energy metabolism offer a clue for the clinical features of patients with CS and provide novel tools valuable for both diagnosis and therapy.

Key words: Cockayne syndrome; DNA oxidation; mitochondrial alteration; oxidative metabolism; oxidative phosphorylation; ROS levels.

Introduction

Mutations in the genes encoding Cockayne syndrome (CS)-A or CS-B are associated with CS, a progeroid disorder characterized by cachectic dwarfism, progressive neurological dysfunction, and precocious aging. CS-A and CS-B are proteins involved in transcription-coupled repair (TCR), a sub-pathway of nucleotide excision repair (NER). However, patients with CS do not present increased cancer risk as expected in DNA repair defective syndromes and show some progeroid features that are difficult to correlate to NER impairment only as they do not occur in XP-A patients, which show a complete NER deficiency (Kraemer *et al.*, 2007). Cockayne syndrome cells are hypersensitive to UV light and also to a variety of oxidizing agents (Pascucci *et al.*, 2011). Whether their sensitivity to oxidative stress accounts for the clinical symptoms and the underlying mechanisms have not been clarified. Cockayne syndrome proteins contribute to the mitigation of the effects of oxidative agents by reducing the load of a variety of oxidative lesions (Tuo *et al.*, 2003; D'Errico *et al.*, 2007; Foresta *et al.*, 2010) in nuclear DNA. This protective function has been ascribed to the ability of CS proteins to stimulate the activity of key base excision repair (BER) enzymes (e.g. Neil1, APE1) (Wong *et al.*, 2007; Muftuoglu *et al.*, 2009) and/or to affect their transcription (e.g. OGG1) (Khobta *et al.*, 2009). However, it is unlikely that the dramatic phenotype of patients with CS is solely because of the role of CS proteins as dispensable co-factors of BER in the removal of nuclear oxidative damage.

A new hypothesis has recently emerged to explain CS pathology, i.e. that CS proteins may be involved in the stability of mitochondria that are the primary source of reactive oxygen species (ROS). Elevated levels of mitochondrial DNA oxidative damage, hypersensitivity to bioenergetic inhibitors as well as altered organization of mitochondrial respiratory complexes have been reported in CS-B mouse cells (Osenbroch *et al.*, 2009). More recently, direct evidence has been provided that in human cells, CS-A and CS-B localize to mitochondria and interact with mitochondrial BER proteins (Kamenisch *et al.*, 2010) playing a direct role in repair by stabilizing repair complexes at the mitochondrial membrane (Aamann *et al.*, 2010).

Here, we show that CS-A and CS-B play a key role in the control of the cellular redox balance, and primary fibroblasts from patients with CS present a significant increased steady-state level of intracellular ROS and decreased basal rates of oxidative phosphorylation (OXPHOS). We also explore the consequences of deregulated ROS production on relevant targets of oxidative stress and provide evidence that oxidative and energy cell metabolism are both affected.

Correspondence
Eugenia Dogliotti, Mariarosaria D'Errico, Istituto Superiore di Sanità, Viale Regina Elena 299, 00161 Rome, Italy. Tel.: 0039 06 49902580; fax: 0039 06 49903650; e-mail: eugenia.dogliotti@iss.it; mariarosaria.derrico@iss.it

*These authors equally contributed to this work.

Accepted for publication *27 February 2012*

Aging Cell

Results

Increased intracellular ROS levels, altered mitochondrial membrane potential, and decreased oxygen consumption characterize CS-A and CS-B primary fibroblasts

Cockayne syndrome primary fibroblasts are hypersensitive to the killing effects of oxidizing agents and accumulate oxidative DNA damage (D'Errico *et al.*, 2007; Ropolo *et al.*, 2007). To test the hypothesis that an altered redox balance might be the underlying mechanism, the bioenergetics status of normal and CS fibroblasts was characterized.

The levels of intracellular ROS in normal and CS primary fibroblasts were measured by using 5-(and-6)-chloromethyl-2′,7′-dichlorodihydrofluorescein diacetate, acetyl ester (CM-H_2DCF-DA) as a probe (Fig. 1A). The conversion of this compound into a fluorescent molecule is proportional to the ROS concentration (Myhre *et al.*, 2003), and it can be monitored by flow cytometry. The steady-state ROS levels were 2-fold higher in primary fibroblasts from both CS-A and CS-B donors as compared to normal ($P < 0.05$; two donors per group). A representative fluorescence profile is illustrated in Fig. 1A. High levels of superoxide anion radicals and/or peroxynitrite in CS cells were also confirmed by using the spin-trap, hydroxy-3-carboxy-pyrrolidine, and electron spin resonance (ESR) analysis (Fig. S1). These data show that CS cells present alterations of the cellular redox balance in physiological conditions.

Mitochondria are the main source of ROS as well as a target of ROS (Van Houten *et al.*, 2006). The mitochondrial membrane potential of the analyzed samples of normal and CS primary fibroblasts was measured by cytofluorimetric analysis using the lipophilic cation probe JC-1 that selectively enters into mitochondria. In this analysis, the cells with high mitochondrial membrane potential fluoresce red (FL2), while those that are depolarized fluoresce green (FL1). Dot-plot of FL2 vs. FL1 resolves cells with intact mitochondrial membrane potential from those with lost membrane potential. A representative profile is shown in Fig. 1B. In the absence of any type of stress, CS-A and CS-B fibroblasts display a 3- to 4-fold increase in the percentage of cells (lower right quadrant) with depolarized mitochondria. The profile of cells treated with the K* ionophore valinomycin, a drug known to affect mitochondrial membrane potential, is shown as a positive control. These data provide evidence of increased loss of mitochondrial membrane potential in CS-A and CS-B fibroblasts in physiological conditions.

To better understand whether CS cells have altered cellular bioenergetics, oxygen consumption, a measure of OXPHOS, was determined using a Seahorse Bioanalyzer. In this experiment, real-time measurements of oxygen consumption are made before and after a pharmacological profile that allows direct assessment of mitochondrial function in intact cells (Figs S2 and S3). All cells were grown in media containing galactose (10 mM), pyruvate (1 mM), and glutamine (2 mM) to drive the cellular bioenergetics toward OXPHOS and away from glycolysis (Rossignol *et al.*, 2004). Under these conditions, CS cells displayed a significant decrease in basal oxygen consumption (Fig. 2A) and ATP-linked oxygen consumption (Figs 2B and S3). The total reserve capacity in CS fibroblasts was similar to normal except for CS1PV (Figs 2C and S3). It would appear that CS cells have the ability to respond to increased ATP demand (Fig. 2C, Sansbury *et al.*, 2011), but maintain lower amounts of ATP production through OXPHOS, as evidenced by the ATP-linked oxygen consumption (Fig. 2B).

Together these data indicate that CS cells present a higher level of intracellular ROS associated with increased frequency of cells with depolarized mitochondria and decreased rate of OXPHOS.

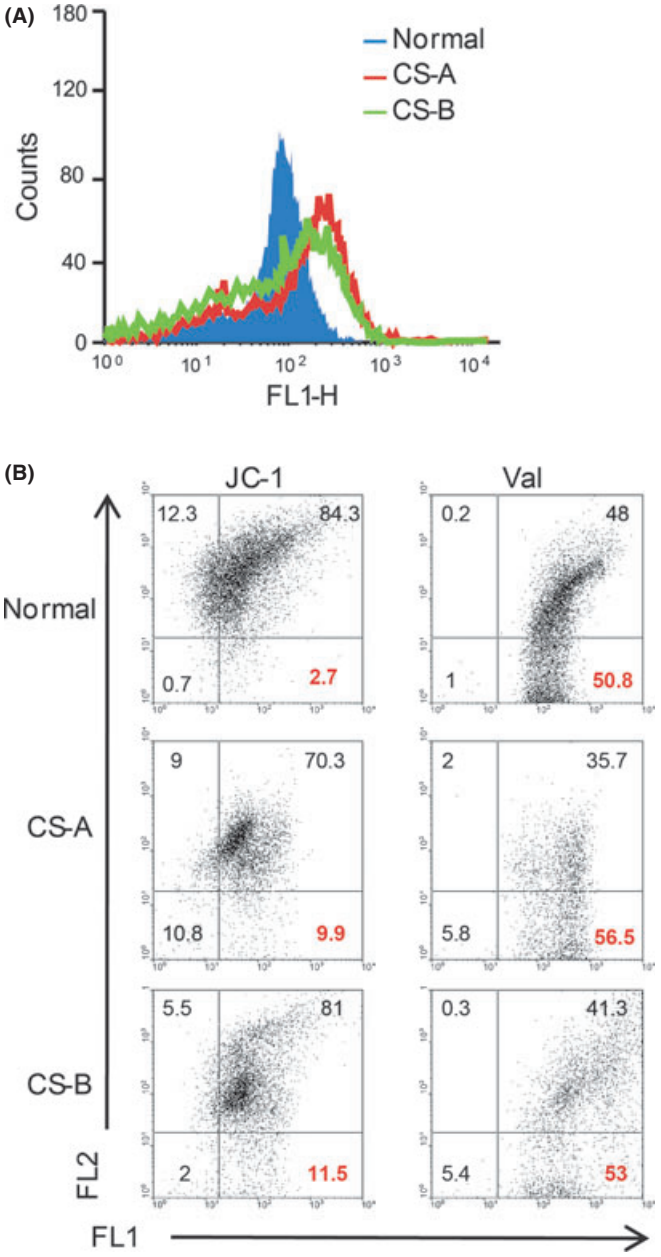

Fig. 1 Cockayne syndrome (CS)-A and CS-B primary fibroblasts present increased levels of intracellular reactive oxygen species (ROS) and decreased mitochondrial membrane potential. (A) Steady-state ROS levels were measured by using the oxidation-sensitive fluorescent probe H_2DCF-DA followed by flow cytometry. In this assay, the production of reactive oxidants is directly proportional to fluorescence intensity. Normal: N2RO; CS-A: CS6PV; CS-B: CS1AN. (B) CS cells are characterized by a loss of mitochondrial membrane potential. Cytofluorimetric analysis of JC-1 stained cells is shown. Cells treated with the K* ionophore valinomycin (val) represent the positive internal control. The amount of depolarized cells is indicated in red. Normal: N2RO; CS-A: CS6PV; CS-B: CS1AN.

^{1}H-NMR metabolic profiles reveal specific metabolic alterations in CS-A and CS-B primary fibroblasts

An increased intracellular ROS concentration and alterations in cellular bioenergetics are expected to affect the cell metabolism. A comparative

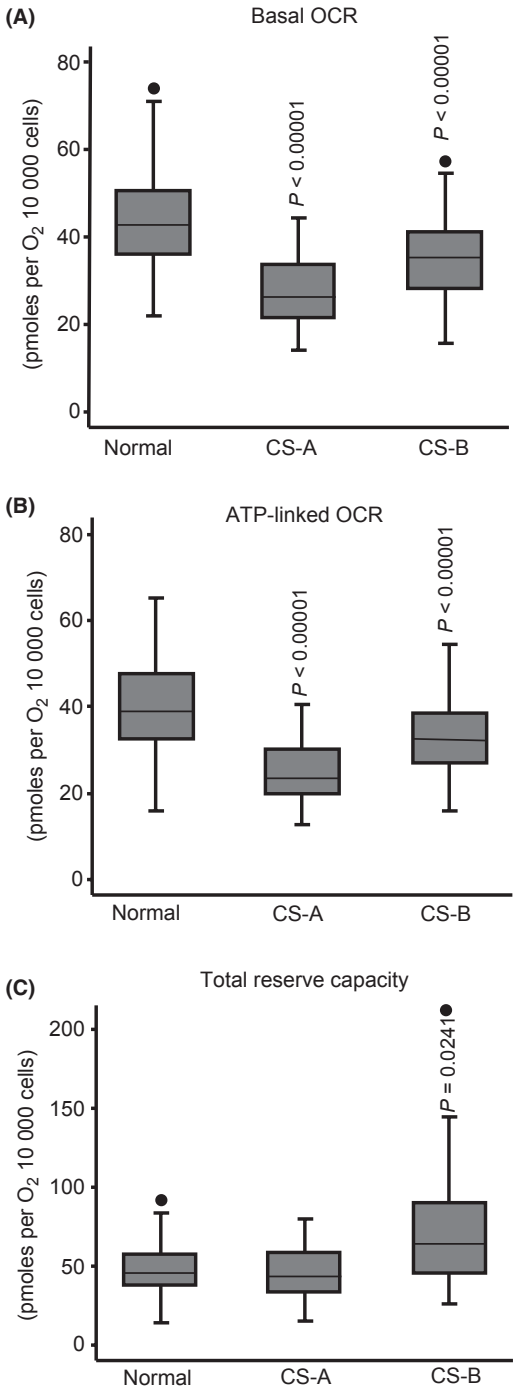

Fig. 2 Cockayne syndrome (CS)-A and CS-B primary fibroblasts have decreased mitochondrial function. Oxygen consumption rates (OCRs) were analyzed using the Seahorse Flux analyzer in two healthy donors (N1RO and N2RO), three CS-A (CS6PV, CS7PV, and CS1JE), and two CS-B (CS1PV and CS12PV) patients. (A) Box plots showing a reduction in basal OCRs in CS fibroblasts. Normal vs. CS-A or CS-B, $P < 0.00001$. (B) Box plots showing a decrease in ATP-linked oxygen consumption CS fibroblasts. WT vs. CS-A or CS-B, $P < 0.00001$. (C) Box plots showing total reserve capacity in normal and CS fibroblasts. Data represent 2–6 independent experiments performed in replicates of 4–6 for each cell strain. Each box encloses 50% of the data. The median of the distribution, the acceptable range, and outliers are indicated. Data were analyzed using a linear mixed effect model; statistical significance was determined by a Wald test. Data for each cell strain are shown in Figs S2 and S3 (Supporting information).

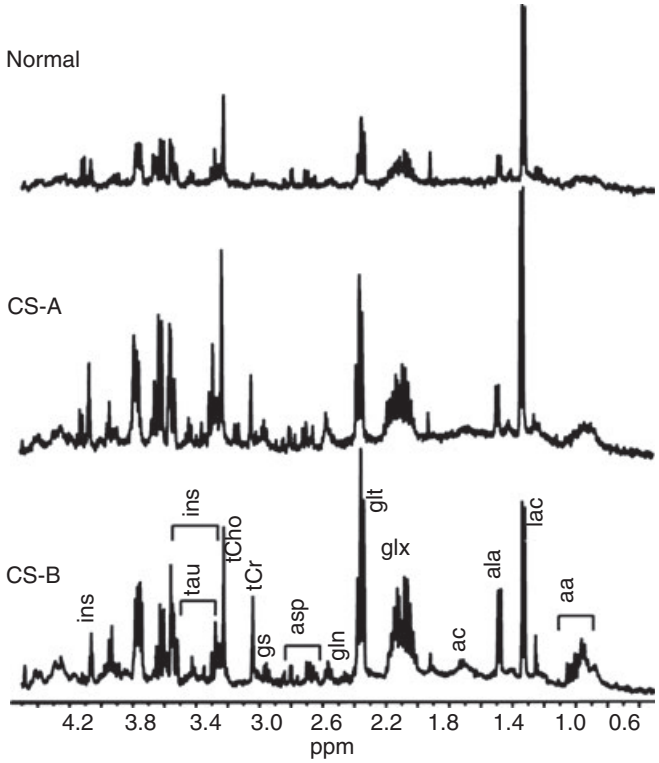

Fig. 3 Cockayne syndrome (CS)-A and CS-B primary fibroblasts are characterized by a perturbed ^{1}H NMR-detected metabolic profile. Representative ^{1}H NMR spectra (400 MHz) of aqueous extracts of normal (N2RO, 1.4×10^6 cells), CS-A (CS6PV, 1.4×10^6 cells), and CS-B (CS1PV, 1.4×10^6 cells) fibroblasts. Peak assignments: aa, (isoleucine, leucine, valine), ala (alanine), asp (aspartate), lac (lactate), ac (acetate), glt (glutamate), gln (glutamine), glx (glutamate + glutamine + glutathione), gs (glutathione), tCr (total creatine: creatine + phosphocreatine), tCho (total choline-containing metabolites) resonance including choline (Cho), phosphocholine (PCho) and glycerophosphocholine (GPCho) as major components, tau (taurine), ins (myo-inositol).

analysis of the metabolic profiles of CS-A, CS-B, and normal fibroblasts was therefore carried out using high-resolution ^{1}H-NMR spectroscopy. To this end, aqueous extracts of primary fibroblasts from three CS-A, two CS-B, and two normal donors (2–7 replicates for each strain) were prepared and analyzed. Examples of the different metabolic profiles of normal, CS-A, and CS-B primary fibroblasts are shown in Fig. 3. As all primary fibroblasts were grown and harvested under the same experimental conditions and the cell volumes were similar, the metabolic profiles can be directly compared among different groups. The concentrations of metabolites of the two normal strains (measured in a total of 11 replicates) did not differ significantly, and their mean values were used as references to estimate the changes in the respective levels of metabolites in the CS strains. Based on the 1D spectra, a total of 16 low molecular weight compounds were identified. Although a certain degree of inter-experiment and inter-strain variability was observed, the levels of a number of metabolites were consistently higher in CS compared with normal cells (Table 1). In particular, the levels of cell osmolytes such as taurine (tau) and myo-inositol (myo-ins) were increased in CS extracts. Moreover, an average threefold increase in the intracellular pool of glutamate (glt and glx) was estimated in CS fibroblasts, suggesting a perturbation in the tricarboxylic acid (TCA) cycle. Metabolites involved in anaerobic glycolysis, such as lactate (lac) and alanine (ala), were also higher in CS compared with normal fibroblasts with an average increase in three to fourfold; a

Table 1 Changes in the levels of ^{1}H NMR-detected metabolites in different CS-A and CS-B strains compared with normal fibroblasts

	CS3BE CS-A (n = 3)			CS7PV CS-A (n = 2)			CS6PV CS-A (n = 2)			CS1AN CS-B (n = 3)			CS1PV CS-B (n = 2)		
	Fold increase†			Fold increase†			Fold increase‡			Fold increase†			Fold increase‡		
Metabolite	Mean	Min–max	t-Test (P)	Mean	Min–max	t-Test (P)	Mean	Min–max	t-Test (P)	Mean	Min–max	t-Test (P)	Mean	Min–max	t-Test (P)
Taurine	6.2	3.8–9.0	< 0.001	3.5	2.9–4.1	0.002	1.6	1.3–2.0	0.107	4.4	3.5–5.9	< 0.001	2.1	2.0–2.1	0.036
Myo-inosytol	3.3	2.2–4.5	0.001	1.7	1.3–2.1	0.057	1.7	1.3–2.0	0.033	3.3	2.4–4.3	0.001	2.0	1.9–2.1	0.005
Glutamate	4.2	2.8–5.4	0.002	2.5	2.3–2.7	0.021	1.7	1.5–1.8	0.057	3.6	2.5–4.5	0.003	3.5	3.0–4.0	0.004
glx	4.2	3.4–4.9	0.002	2.1	1.8–2.4	0.053	1.6	1.5–1.6	0.061	3.8	2.8–4.7	0.003	3.0	2.8–3.2	0.004
Lactate	6.1	5.6–7.1	0.001	1.6	1.4–1.7	0.120	1.4	0.9–1.9	0.225	4.2	3.2–5.9	0.002	2.5	2.1–2.9	0.039
Alanine	3.7	3.0–4.7	0.004	2.2	0.9–3.5	0.129	1.8	1.6–1.9	0.007	2.6	1.9–3.2	0.013	2.7	2.4–3.0	0.001
Valine	4.8	3.8–6.5	0.002	1.8	1.4–2.1	0.091	1.8	1.6–2.1	0.016	4.6	2.7–5.8	0.003	3.1	2.8–3.4	0.001
Iso-leucine	4.3	2.8–6.4	0.003	2.1	2.0–2.1	<0.05	2.2	1.4–3.0	0.039	4.6	2.8–5.6	0.002	3.6	2.8–4.4	0.004
PCho	3.2	2.5–4.0	0.002	1.8	1.0–2.5	0.114	0.8	0.2–2.4	0.719	2.4	2.2–2.6	0.006	2.4	2.4–2.5	0.035

CS, Cockayne syndrome; n = number of replicates for each CS strain; glx, glutamate + glutamine + glutathione; PCho, phosphocholine.
t-Test (one tailed) was performed on the log-transformed metabolite concentrations (nmol10^6 cells).
†Fold increase vs. six replicates in normal cell lines.
‡Fold increase vs. five replicates in normal cell lines.

similar increase was observed for valine (val) and isoleucine (iso-leu). Regarding the total pool of choline-containing metabolites (tCho), we observed a trend for increased levels in CS compared to normal cells (data not shown), with a statistically significant difference only for phosphocholine (PCho) in some strains (Table 1). Other metabolites such as acetate, glutathione, and aspartate were not different between the CS and normal cells. As shown in Table 1, we found a statistically significant increase in the content of these metabolites in the CS-B cells analyzed, while in CS-A cells, although there was a trend toward increased values, the differences were not always significant.

We can conclude that the functional inactivation of either *CS-A* or *CS-B* is associated with similar changes in the absolute concentrations of individual metabolites belonging to several pathways, namely glycolysis, oxidative metabolism, choline phospholipid metabolism, and osmoregulation. These metabolic differences allow clear discrimination of CS from normal fibroblasts and may act as possible fingerprints for the pathological status.

The treatment with an antioxidant reduces the ROS levels and changes the metabolic profile of CS cells

If increased oxidative stress leads to the metabolic impairment of CS fibroblasts, the expectation is that the reduction in the ROS levels could ameliorate the metabolic defect. Cells were grown in the presence of the antioxidant N-acetyl cysteine (NAC) (5 mM for 8 days), and the levels of ROS were measured by using CM-H_2DCF-DA as a probe. In the presence of the antioxidant, a significant reduction in ROS levels in CS-A and CS-B fibroblasts as well as in normal cells was observed (Fig. 4A). Antioxidant treatment for 8 days prior to metabolic assessment partially reverted also the metabolic profile of CS-A and CS-B cells, as shown by the consistent reduction in the concentrations of specific metabolites to levels similar to those of normal cells (Fig. 4B). This is consistent with the hypothesis that the continuous oxidative stress that characterizes CS cells plays a causative role in the underlying physiology.

Reduced levels of Na/K-ATPase characterize CS cells

A relevant target of oxidative stress is represented by Na/K-ATPase, a membrane protein crucial for maintaining cell homeostasis (McKenna

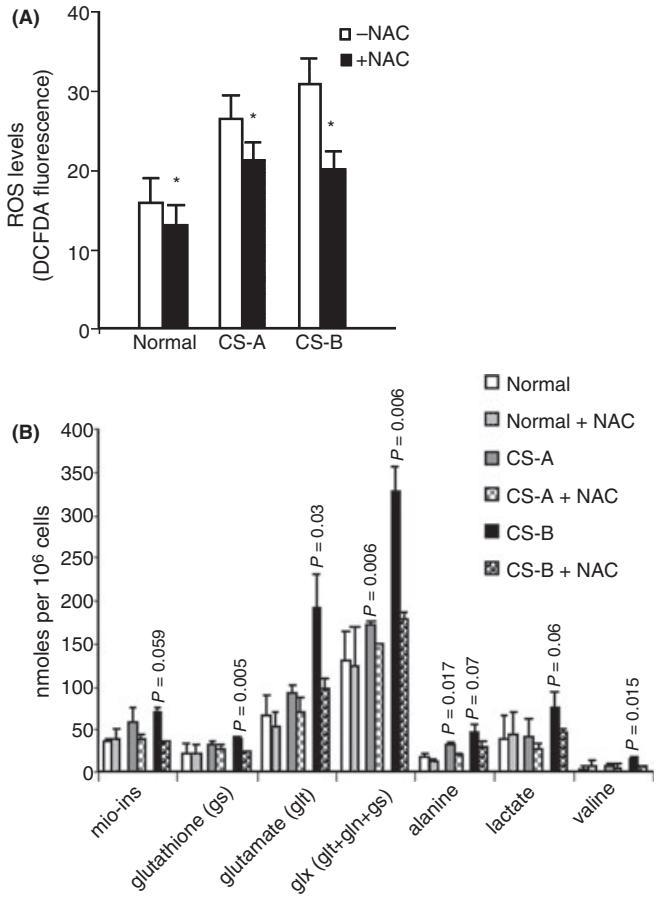

Fig. 4 N-acetyl cysteine (NAC) treatment reduces the oxidative stress in CS cells. (A) Intracellular reactive oxygen species (ROS) levels as assessed by DCFDA fluorescence intensity (arbitrary units) were measured after NAC treatment (5 mM) for 8 days. ROS measurements were made from three independent experiments. The reported values are the means ± SD (*$P \leq 0.05$). (B) Changes in the contents of some metabolites in normal and CS cells after NAC treatment. The reported values are the means of three independent experiments ± SD. Normal: N2RO; CS-A: CS6PV; CS-B: CS1PV.

et al., 2006). The Na/K-ATPase is also one of the highest consumers of cellular ATP (Buttgereit & Brand, 1995; Wieser & Krumschnabel, 2001). The total cell pool of beta Na/K-ATPase protein in primary fibroblasts from normal, CS-A and CS-B donors was therefore compared. Representative results are shown in Fig. 5A. Similar cellular amounts of the protein were observed in normal subjects whereas 30–60% lowered beta Na/K-ATPase levels were present in fibroblasts from patients with CS-A and CS-B. The reduction was statistically significant for both CS groups ($P < 0.005$), indicating that CS-specific alterations are paralleled by a remarkable decrease in Na/K-ATPase levels. When the levels of Na/K-ATPase mRNAs were measured, the levels of transcripts were consistently lower in CS fibroblasts as compared to normal fibroblasts (Fig. 5B).

To unequivocally demonstrate the link between CS-A or CS-B inactivation and Na/K-ATPase reduction, we evaluated the amount of beta Na/K-ATPase in the SV-40 transformed CS-A (CS3BE) and CS-B (CS1AN) cell lines and in their isogenic derivatives expressing the corresponding wild-type gene. As shown in Fig. 5C, a statistically significant ($P < 0.001$) increase in Na/K-ATPase levels was observed in cells expressing normal CS-A or CS-B protein compared to the parental mutant cell lines. These findings indicate that the loss of functional CS-A and CS-B proteins results in a decreased level of Na/K-ATPase. Thus, in CS cells, the aberrant ROS production and altered redox status are associated with the depletion of this ATP-consuming process.

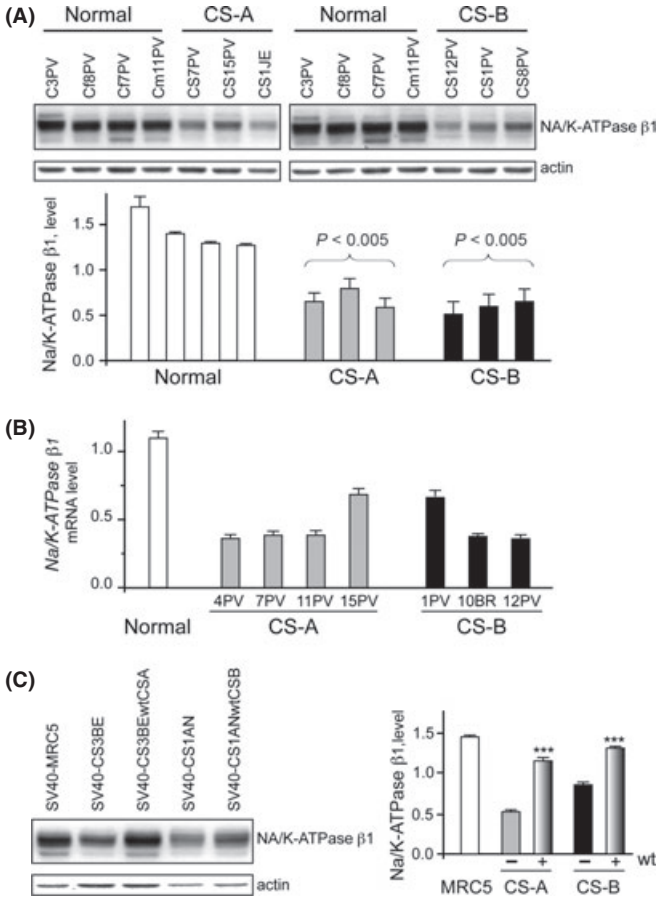

Fig. 5 Cockayne syndrome (CS)-A and CS-B cells present reduced levels of NA/K-ATPase that are reversed by complementation. (A) NA/K-ATPase β1 immunoblot analysis and, (B) mRNA levels of primary fibroblasts from normal and CS donors; (C) NA/K-ATPase β1 immunoblot analysis of normal (MRC5), CS-A (CS3BE) and CS-B (CS1AN) SV40-trasformed fibroblasts, and their isogenic derivatives expressing the wild-type genes (CS3BEwtCS-A and CS1ANwtCS-B). The NA/K-ATPase β1 amounts were normalized to the actin content. The reported values are the means of three independent experiments ± SE (***$P < 0.001$).

As the Na/K-ATPase is one of the major ATP-consuming processes in the cell, steady-state ATP levels in normal and CS fibroblasts were measured. Cockayne syndrome cells showed significantly higher steady-state levels of ATP (Fig. S4). This finding together with the previous observation of decreased OXPHOS, as evidenced by decreased basal and ATP-linked oxygen consumption rates (OCRs) (Fig. 2B), indicates that the rates of ATP consumption are considerably lowered in CS cells.

The level of oxidative DNA damage in CS fibroblasts reflects an altered redox balance

To understand how an alteration in the redox balance would impact on the level of basal oxidative DNA damage, 8-oxoguanine (8-OH-Gua) residues were measured in both mitochondrial (mt) and nuclear (n) DNA by HPLC-ED of normal and CS fibroblasts. As shown in Fig. 6A, the levels of oxidation of mtDNA were higher than those of nDNA (approximately two fold higher). Similar levels of 8-OH-Gua were observed in normal and CS cells when comparing mtDNAs, whereas a trend toward higher basal levels of 8-OH-Gua was observed in nDNA from CS fibroblasts (D'Errico *et al.*, 2007). The presence of NAC in the culture medium resulted in lower oxidation levels in all the analyzed cell samples, indicating that DNA oxidation reflects the local ROS concentration.

The increased basal levels of nDNA oxidation observed in CS cells prompted us to investigate whether the response to induced oxidative stress was also affected. Upon exposure to 200 μM H_2O_2, CS cells showed higher levels of intracellular ROS (Fig. S5, panel A) and increased frequency of cells with depolarized mitochondria (Fig. S5, panel B) as compared to normal fibroblasts. Normal and CS primary and SV-40 transformed fibroblasts were then exposed to a range of H_2O_2 doses 15 min on ice to prevent repair, and oxidative DNA damage was measured (Fig. 6B–D). In this range of doses, CS cells were hypersensitive to H_2O_2 as measured by a clonal assay (Fig. S6). DNA damage was quantified by measuring DNA single-strand breaks (SSB) including those arising from abasic sites by the comet assay (Fig. 6B). Both CS and normal cells present a statistically significant ($P < 0.01$) dose-dependent increase in the DNA break level expressed as tail moment (TM). Notably, the level of SSB is significantly higher ($P < 0.05$) in CS-A and CS-B primary fibroblasts compared to normal at the highest dose tested (100 μM) (Fig. 6B) and it is partially but significantly reduced upon expression of the wild-type genes (50 and 75 μM, $P < 0.01$) in the SV-40 transformed CS-A and CS-B cells (Fig. 6C). To ascertain whether the effects observed were because of ROS induction, DNA oxidation was measured by HPLC-ED in cells maintained for 8 days in the presence of NAC. The pretreatment with the antioxidant drastically reduced the levels of both basal and H_2O_2-induced DNA base oxidation (Fig. 6D) indicating that these processes are mediated by ROS production. A trend toward increased levels of both basal and induced DNA damage in CS as compared to normal cells was also observed (Fig. 6D).

All together these results indicate that both the spontaneous and induced DNA oxidation are affected by the intracellular ROS levels (NAC inhibited). Inactivation of CS proteins leads to altered redox status that causes accumulation of nuclear DNA damage and likely accounts for increased cell killing.

Discussion

A large body of evidence indicates that upon oxidative stress, CS-A and CS-B cells show increased cytotoxicity and accumulate a variety of

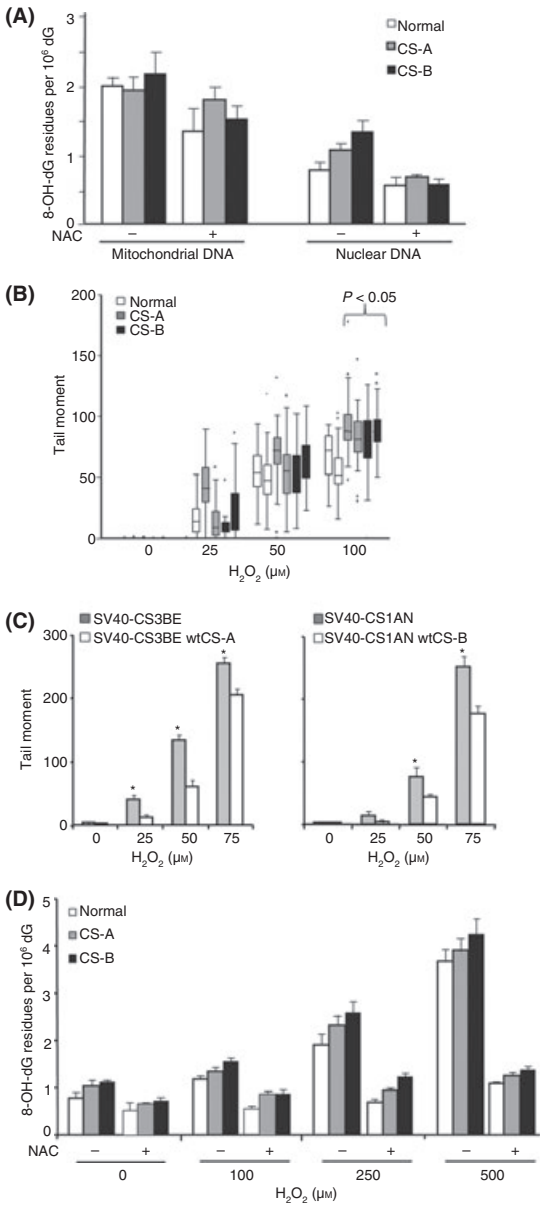

Fig. 6 Cockayne syndrome (CS)-A and CS-B cells present increased levels of oxidative stress-induced DNA damage that are reversed by complementation and by pretreatment with N-acetyl cysteine (NAC). (A) Basal levels of 8-oxo-Gua in mitochondrial and nuclear DNA were measured by HPLC-ED in normal and CS primary fibroblasts from normal and CS donors after NAC treatment incubated in the absence or presence of NAC (5 mM for 8 days). Experiments were performed in duplicate. Normal: N2RO; CS-A: CS6PV; CS-B: CS20PV. (B) Cells were exposed to different doses of H_2O_2 for 15 min on ice, and SSB were measured by the comet assay in normal and CS primary fibroblasts from normal and CS donors exposed to different doses of H_2O_2 for 15 min on ice. Normal: N1RO and N2RO; CS-A: CS6PV and CS7PV; CS-B: CS1PV and CS1AN. Data from three independent experiments are reported as box plots. Each box encloses 50% of the data. The median of the distribution, the acceptable range and outliers are indicated. (C) Comet assay was performed on CS-A SV40-CS3BE and CS-B SV40-CS1AN transformed fibroblasts, and their isogenic derivatives expressing the wild-type genes (SV40-CS3BEwtCS-A and SV40-CS1ANwtCS-B). Means of three independent experiments ± SE are reported; $*P < 0.01$ by nonparametric Wilcoxon ranksum test. (D) Modulation of H_2O_2-induced nuclear 8-oxo-Gua levels by NAC pretreatment of normal and CS primary fibroblasts from normal and CS donors exposed to different doses of H_2O_2 for 15 min on ice. Experiments were performed in duplicate. Normal: N2RO; CS-A: CS6PV; CS-B: CS20PV.

oxidative base lesions (reviewed in Pascucci *et al.*, 2011) including DNA SSB (this study). However, the mechanistic role of CS proteins in the control of oxidative damage is not clearly understood. In this study, we provide the first evidence that CS-A and CS-B primary fibroblasts present an altered redox balance, changes in cellular bioenergetics, and alterations in cellular metabolism. We further demonstrate that the addition of an antioxidant partially reverts the physiological impairment, suggesting that oxidative stress plays an important pathophysiological role.

Partially disassembled complexes of the inner mitochondrial membrane have been reported in CS-B mutant mice together with hypersensitivity to bioenergetic inhibitors and impaired ability to recover from cellular ATP depletion (Osenbroch *et al.*, 2009). Here, we show that primary fibroblasts from patients with CS-A and CS-B, even in the absence of stress, present a reduction in the mitochondrial membrane potential (Fig. 1) and oxygen consumption through OXPHOS (Fig. 2). Cells containing depolarized mitochondria are expected to be susceptible to apoptosis (Dörrie *et al.*, 2001). Indeed CS proteins have been shown to be protected from mitochondrial DNA mutations and apoptosis-mediated loss of subcutaneous fat in a mouse model of CS (Kamenisch *et al.*, 2010). We speculate that CS cells lower their demand for ATP by decreasing the levels of Na/K-ATPase and decreasing the rate of basal oxygen consumption as a strategy to maintain low levels of mitochondrial ROS that would otherwise cause increased mitochondrial DNA damage, which cannot be efficiently repaired in CS cells (Kamenisch *et al.*, 2010).

The increased intracellular ROS concentration that we observed in CS fibroblasts is compatible with damage to mitochondria although we cannot exclude other ROS sources. Alternative candidates for ROS production are enzymes metabolizing oxygen in the vicinity of nuclear DNA, such as lipooxygenases, NAD(P)H oxidases, xanthine oxidases, and cytochromes that are located in the membrane of the nucleus. In this regard, it is interesting to note that Newman *et al.* (2006) found higher levels of pro-inflammatory mediators such as expression of NCF2, a gene encoding for the neutrophil cytosolic factor 2 subunit of NADPH oxidase, in a CS-B cell line (as revealed by our re-evaluation of published data). Moreover, activation of another subunit of NADPH oxidase (NOX1) has been reported upon silencing of XPC in human keratinocytes resulting in more ROS production and accumulation of mitochondrial mutations (Rezvani *et al.*, 2011). Future research should address the role of these ROS-producing systems in DNA repair defective human syndromes.

One question that arises is what are the consequences of an altered redox status?

We show that the altered redox status that characterizes CS cells leads to accumulation of nuclear DNA damage (that is efficiently inhibited by the antioxidant NAC), and this is likely to account for hypersensitivity to oxidative stress.

As expected for an ATP-consuming process, under excessive ROS production, the Na/K-ATPase is inhibited (McKenna *et al.*, 2006 and references therein). We are tempted to speculate that the Na/K-ATPase might belong to the set of genes whose transcription is selectively influenced, after damage, in CS-B cells (Frontini & Proietti-De-Santis, 2009).

Changes in the intracellular redox status are expected to affect the oxidative and energy metabolism, and we provide evidence that this indeed occurs in CS fibroblasts. The ^{1}H-NMR profile of CS-A and CS-B primary fibroblasts shows a significant increase in glutamate concentrations as compared to normal cells. The high level of glutamate is expected to lead to a reduction in alpha-ketoglutarate with an impact on the TCA cycle efficiency (Tiziani *et al.*, 2009). The increase in cellular valine and isoleucine content, as detected in CS metabolic profiles, might be a consequence of this impairment (reviewed in Ott *et al.*, 2005). Interestingly, an

interaction of CS-B with 3-hydroxyisobutylryl-coenzymeA hydrolase (HIB-CoA) that belongs to the valine catabolic pathway has been recently reported (Aamann *et al.*, 2010), suggesting that CS proteins might also play a direct role in aminoacid catabolism. In response to a decline in OXPHOS, a concomitant increase in glycolysis might be expected to occur, as actually confirmed by the observed 3- to 5-fold increases in lactate and alanine in CS cells. The phosphocholine accumulation detected in some CS fibroblasts could be derived from altered beta-oxidation of fatty acids in these cells characterized by mitochondrial impairment (Farber *et al.*, 2000). The metabolic profile of CS cells also revealed an increase in taurine and myo-inositol levels, two compounds with anti-oxidant properties and both exerting an osmoregulatory function.

The overall metabolic profile of CS cells can be significantly reverted by the addition of an antioxidant suggesting that the perpetuating cycle of mitochondrial damage and oxidative stress identified by this study plays a causal role in the pathophysiology of CS cells. Interestingly, this 'vicious cycle' is thought to contribute to aging (van der Pluijm *et al.*, 2007; Page *et al.*, 2010) and mediates the physiological impairment induced by the disruption of autophagy (Wu *et al.*, 2009). It is also of note that the metabolic profiles of CS primary fibroblasts show alterations in the excitatory amino acid metabolism, changes in the levels of neurotransmitters, and perturbation of osmoregulation. The deregulation of these processes may contribute to some of the clinical features of CS, such as premature aging and neurodegeneration. Patients with a deficiency in the valine catabolic pathway, such as that we have highlighted in CS fibroblasts, present with hypotonia, motor delay, and subsequent neurological regression (Loupatty *et al.*, 2007). Furthermore, many of the ultimate manifestations of neurodegenerative mitochondrial diseases are triggered by a metabolic imbalance characterized by accumulation of lactate (reviewed in Mancuso *et al.*, 2009) similar to that observed in CS fibroblasts.

In conclusion, this study provides the first evidence of altered redox balance and changes in cellular bioenergetics in primary fibroblasts from patients with CS-A and CS-B. The associated alterations of oxidative and energy metabolism might account for some of the clinical features of patients with CS and unveil new potential biomarkers for the diagnosis, prognosis, and potential treatment of this devastating multisystem disease.

Experimental procedures

Cell cultures and treatment

Experiments were performed on primary fibroblast cultures obtained from biopsies from unaffected skin areas of CS-A [CS3BE (GM01856; Coriell Cell Repository, Camden, NJ, USA), CS1JE, CS6PV, CS7PV and CS15PV] and CS-B [CS1AN (GM00739; Coriell Cell Repository), CS1PV, CS8PV, CS12PV, CS20PV and CS10BR] patients, and six healthy donors (N1RO, N2RO, C3PV, Cf8PV, Cf7PV and Cm11PV). We also used SV40-transformed MRC5 (normal), CS1AN (CS-B), and CS3BE (CS-A) cell lines and their isogenic derivatives expressing the wt CS genes. Cell strains and lines were cultured as previously described (D'Errico *et al.*, 2005). Treatments with H_2O_2 were performed in DMEM (Invitrogen, Carlsbad, CA, USA) supplemented with 20 mM Hepes. Treatments with 5 mM NAC were performed in DMEM supplemented with 10% fetal bovine serum for 8 days. The CS1ANwtCS-B cell line was a gift of Dr. Hoeijmakers JH, Rotterdam, NL. Cell survival was determined by analyzing the colony-forming ability, as described previously (D'Errico *et al.*, 2005). Colonies were fixed 14 days later. The number of colonies in treated cells was expressed as a percentage of that in untreated cells.

Analysis of DNA breakage

Primary and SV-40 transformed fibroblasts were treated with different doses of H_2O_2 (up to 100 μM) for 15 min on ice to avoid repair and then subjected to the comet assay as previously described (Fortini *et al.*, 1996). DNA break levels were compared by nonparametric Wilcoxon ranksum test. The level of heterogeneity between mean values in different donor groups was assessed by a one-way analysis of variance. Because of differences in the morphology and migration response to damage of transformed and primary fibroblasts, the tail moments cannot be compared between these different cell types (Tice *et al.*, 2000).

Measurement of 8-OH-Gua by HPLC-ED

Repair of 8-OH-Gua lesions was determined by HPLC-ED according to established procedures (Cappelli *et al.*, 2000). Briefly, enzymatic digestion of DNA was accomplished at 37 °C with nuclease P1 (Boehringer Mannheim) and alkaline phosphatase (Boehringer Mannheim) for 2 h. Aliquots of the DNA hydrolyzate were analyzed on a LC18-DB column (250 mm by 46 mm, 5-μm; Supelco; Sigma-Aldrich S.r.l., Milan, Italy), equipped with a C18 μ guard column. The separation was isocratic with 50 mM ammonium acetate, pH 5.5, with 10% methanol, at a flow rate of 1.0 mL min^{-1}. The HPLC device (Beckman, System Gold) was equipped with a UV detector (256 nm) and an Electrochemical detector (Coulochem II; ESA Inc., Chelmsford, MA, USA) with applied potentials at 150 and 300 mV for E1 and E2, respectively. 2′-Deoxyguanosine was measured in the same run of corresponding 8-OH-Gua, and the results are expressed as the number of 8-OH-Gua residues/10^6 Gua residues.

Intracellular ROS levels

Intracellular concentration of ROS was determined using the oxidation-sensitive fluorescent probe, 5-(and-6)-chloromethyl-2′,7′-dichlorodihydrofluorescein diacetate, acetyl ester (CM-H_2DCF-DA; Invitrogen, Molecular Probes, Eugene S.r.l., Milan, Italy) and detected by flow citometry. Primary fibroblasts were incubated for 30 min with 5 mM H_2DCF-DA, washed once with PBS, treated with H_2O_2, harvested and immediately analyzed by flow cytometry. The observation of increased intracellular ROS levels in CS fibroblasts was confirmed by EPR analysis. The spin probe 1-Hydroxy-3-Carboxy-Pyrrolidine (CPH; 1 mM) was added to 2×10^6 cells mL^{-1} in phosphate buffer, pH 7.4. Samples were drawn up into a gas-permeable Teflon tube and inserted into a quartz tube. EPR spectra were measured in air at 37 °C on a Bruker ECS 106 spectrometer (Bruker, Rheinstetten, Germany) equipped with a variable-temperature unit (ER4111VT) and a ESR cavity (4108 TMH). Spectrometer conditions common to all spectra were as follows: modulation frequency, 100 kHz; microwave frequency, 9.4 GHz; microwave power, 20 mW; gain 1×10^4; modulation amplitude, 0.1 mT; conversion time, 20.5 ms; time constant, 82 ms; sweep time, 21 s; number of scans, 1.

Measurement of mitochondrial function

Oxygen consumption rate was made with a Seahorse XF24-3 Extracellular Flux Analyzer (Seahorse Bioscience, Billerica, MA, USA). The Seahorse Bioscience XF24 Extracellular Flux Analyzer measures OXPHOS in real time (Qian & Van Houten, 2010). The cartridge contains a fluorophore that is sensitive to changes in oxygen concentration and measures the OCR, which enables it to accurately measure the rate at which cytochrome c oxidase (complex IV) reduces one O_2 molecule to two H_2O molecules during OXPHOS. Cells were cultured in DMEM supplemented with dialyzed

10% FBS, 1 mM pyruvate, 2 mM glutamine, and 10 mM galactose for 48 h and were seeded in 24-well Seahorse tissue culture microplates in at a density of 4×10^4 cells per well and incubated overnight at 37 °C. Before running the Seahorse assay, cells were incubated for 1 h without CO_2, in DMEM unbuffered media containing all the same components except 10%FBS. Real-time automated measurements were performed prior to and after the injection of four compounds affecting bioenergetic capacity: oligomycin (1 μM) injection 1, FCCP (300 nM) at injection 2, 2-DG (100 mM) at injection 3, and rotenone (1 μM) at injection 4. Experiments were performed in real time in 4–6 replicate wells for each cell strain. Each cell strain was analyzed by the Seahorse in 2–6 independent experiments. Total wells for each cell strain over all the experiments were analyzed statistical analysis using STATA/SE 12 (Stata Corp LP, College Station, TX, USA) statistical software. The comparisons of basal OCR, total reserve capacity, and ATP-linked OCR between different groups of cell strains were performed using linear mixed effect models using a Wald test. $P < 0.05$ was considered statistically significant. The basal level of OCR was calculated by the difference between the mean of time point rates at 1–4 and the mean of rates 14–16. ATP-coupled respiration is the initial basal rate of oxygen consumption (mean of times points 1–4) minus the time points after oligomycin injection (mean of point 4–6). The total reserve capacity was calculated by the difference between the mean of OCR rates 11–13 and the mean of rates 14–16. Data were reported in pmol min^{-1} for OCR. After the completion of the experiment, cells were immediately trypsinized and counted with the CASY Cell Counter (Innovatis, Bielefeld, Germany) to normalize individual well-rate data to cell counts.

Measurement of steady-state ATP levels

The ATPlite ATP Luminescence Detection Assay System (PerkinElmer, Waltham, MA, USA) quantifies steady-state ATP levels based on luminescence produced by an ATP-dependent luciferase reaction (Qian & Van Houten, 2010). Briefly, 20 000 cells per well were grown overnight in a 96-well black microplate in DMEM supplemented with 10% FBS, 1 mM pyruvate, 2 mM glutamine, and 10 mM galactose. The resulting luminescence was measured using a Biotek Synergy 2 Plate Reader (Winooski, VT, USA) and compared to a series of ATP standards to determine ATP concentration.

Mitochondrial membrane potential

Primary fibroblasts were treated with H_20_2 (200 μM) for 20 min and then stained for 30 min in the dark with 1 mg mL^{-1} of the lipophilic cation 5,5′,6,6′-tetrachloro-1,1′,3,3′-tetraethybenzimidazolcarbocyanineiodite (JC-1; Invitrogen, Molecular Probes). After two washes with ice-cold PBS, cells were immediately analyzed in the EPICS XL-MCL flow cytometer. A positive control sample, obtained by adding 100 nM valinomycin (a well-known $K^{\bullet}$ionophore), was included in each experiment.

NMR spectroscopy

Primary fibroblasts grown to 60–70% confluence were trypsinized 24 h after culture medium change, counted, and assessed for cell viability (80–90%) and membrane integrity by trypan blue staining. Cells were washed twice with ice-cold physiological saline solution and pellets resuspended in 0.5 mL of ice-cold twice-distilled water. Aqueous extracts (from 5 to 10×10^6 cells per sample) were prepared in EtOH 70% according to an established protocol (Iorio *et al.*, 2005). Briefly, samples were ultra-sonicated at 20 kHz by a MSE ultrasonic disintegrator Mk2 (Crawley Sussex, UK) and centrifuged at 14 000 *g* for 30 min. Supernatants were lyophilized twice in a RVT 4104 Savant lyophilizer (Mildford, ME, USA), and the residue resuspended in 0.7 mL D_2O (Sigma-Aldrich, St. Louis, MO, USA) containing 0.1 mM 3-(trimethylsilyl)-propionic-2,2,3,3-d4 acid sodium salt (TSP) as internal chemical shift and peak area standard. High-resolution NMR experiments (25 °C) were performed at 9.4T (Bruker AVANCE spectrometer, Karlsruhe, Germany). ^{1}H-NMR spectra of cell extracts were acquired using 90° flip angle, 30 s repetition time, 32K time domain data points, and 128 transients (Iorio *et al.*, 2005). Measurement of protein content by standard procedure showed similar levels in normal and defective cells. In particular, the protein contents were found to be 0.19 ± 0.01 mg protein per 10^6 cells for wild-type fibroblasts, 0.17 ± 0.02 mg protein per 10^6 cells for CS-A and 0.22 ± 0.01 mg protein per 10^6 cells for CS-B fibroblasts.

Analysis of NA/K-ATPase protein and transcript levels

Samples of 3×10^5 fibroblasts were resuspended in 200 μL of RIPA buffer [50 mM Tris-HCl pH 7.4, 150 mM NaCl, 1% Triton X-100, 1% Na-deoxycholate, 0.1% sodium dodecyl sulfate (SDS), 2 mM EDTA, protease inhibitors (Complete Mini; Roche Diagnostic GmbH, Mannhein, Germany), and phosphatase inhibitors (PhosStop, Roche), sonicated three times for 10 s on ice, and stored at –20 °C. About 15 μg of proteins per sample were resolved on 12% polyacrylamide-SDS gels and transferred onto nitrocellulose membranes (Protran, Schleicher and Schuell, Dassel, Germany). The membranes were blocked in 5% skim milk for 1 h and incubated overnight at 4 °C with primary antibodies against Na/K-ATPase beta subunit (ab2873; Abcam, Cambridge, UK) or actin (A2066; Sigma) diluted in blocking buffer. The signals were detected with secondary antibodies (Jackson Immuno Research Laboratories, West Grove, PA, USA) conjugated to horseradish peroxidase by using the Chemiluminescent substrate (Pierce, Thermo Scientific, Rockford, IL, USA). Chemiluminescence signals corresponding to the different antibodies were acquired with a cooled CCD camera (ChemiDoc XRS; Bio-Rad Laboratories, Hercules, CA, USA) and the density of the bands quantified using the IMAGEJ 1.34s software (Wayne Rasband, National Institutes of Health, Bethesda, MD, USA). RNA extraction was performed according to the manufacturer's instructions for the RNeasy Kit (Qiagen S.r.l., Milan, Italy). In a single RT reaction, 1 μg of RNA was retro-transcribed by using the iScript cDNA Synthesis Kit (Bio-Rad). The cDNAs were diluted 1:10 in water, and 4 μL were used as template in 16 μL real-time PCR containing 10 pmol each forward and reverse primers. The following primers were used: 5′-TGCCTCATAGCTCTT-3′ (forward) and 5′-GCTGCTCACCATCAGTGAAT-3′ (reverse) for the NA/K-ATPase amplicon, 5′-GTTGTCGACGACGAGCG-3′ (forward) and 5′-GCACAGAGCCTCGCCTT-3′ (reverse) for the β actin amplicon. The real-time PCR were performed using the iQ SYBR Green Supermix (Bio-Rad) and by activation of Taq polymerase at 95 °C for 15′, followed by 40 three-step amplification cycles consisting of 25″ denaturation at 95 °C, 25″ annealing at 60 °C and 25″ extension at 72 °C. A final dissociation stage was run to generate a melting curve for verification of amplification product specificity. The reactions were monitored and analyzed by the LightCycler 480 (Roche). All samples, including the external standards and nontemplate controls, were run in triplicate.

Acknowledgments

We are grateful to Dr. Donatella Pietraforte and Dr. Paola Fattibene (Istituto Superiore di Sanità, Rome, Italy) for performing the EPR anal-

ysis of ROS levels. We would like to thank Dr. Donata Orioli (CNR, Pavia, Italy) for the analysis of Na/K-ATPase mRNA levels and helpful discussion. We would like to thank Lucas Santana dos Santos (Univ. of Pittsburgh, Pittsburgh, USA) for the analysis of gene expression data sets. This work was supported by Associazione Italiana per la Ricerca sul Cancro, Fondazione Cariplo, Programma Malattie Rare (Institute of Public Health), Progetto Integrato Oncologia (Ministry of Public Health), and a grant with the Pennsylvania Department of Health, the PA CURE (BVH). The research leading to these results has received funding from the European Atomic Energy Community's Seventh Framework Programme (FP7/2007–2011) under grant agreement no 249689.

Author contributions

TL, SG and LN performed cell and molecular biology experiments; EI and FP were involved in the NMR experiments and data interpretation; BV performed the molecular analysis of Na/K-ATPase; II carried out statistical analysis; AC gave technical support; PD was involved in the HPLC-EC experiments; VR performed cell culturing and seahorse experiments; BVH analyzed Seahorse experiments data and contributed to manuscript writing; BMJ provided statistical analysis of the Seahorse data; BP performed experiments and contributed to data interpretation and manuscript writing; MS was involved in data interpretation and manuscript writing; ED designed the study and wrote the manuscript; MD designed and coordinated the study, performed experiments and wrote the manuscript.

References

Aamann MD, Sorensen MM, Hvitby C, Berquist BR, Muftuoglu M, Tian J, de Souza-Pinto NC, Scheibye-Knudsen M, Wilson DM 3rd, Stevnsner T, Bohr VA (2010) Cockayne syndrome group B protein promotes mitochondrial DNA stability by supporting the DNA repair association with the mitochondrial membrane. *FASEB J.* **24**, 2334–2346.

Buttgereit F, Brand MD (1995) A hierarchy of ATP-consuming processes in mammalian cells. *Biochem J.* **312**, 63–67.

Cappelli E, Degan P, Frosina G (2000) Comparative repair of the endogenous lesions 8-oxo-7, 8-dihydroguanine (8-oxoG), uracil and abasic site by mammalian cell extracts: 8-oxoG is poorly repaired by human cell extracts. *Carcinogenesis* **21**, 1135–1141.

D'Errico M, Teson M, Calcagnile A, Nardo T, De Luca N, Lazzari C, Soddu S, Zambruno G, Stefanini M, Dogliotti E (2005) Differential role of transcription-coupled repair in UVB-induced response of human fibroblasts and keratinocytes. *Cancer Res.* **65**, 432–438.

D'Errico M, Parlanti E, Teson M, Degan P, Lemma T, Calcagnile A, Iavarone I, Jaruga P, Ropolo M, Pedrini AM, Orioli D, Frosina G, Zambruno G, Dizdaroglu M, Stefanini M, Dogliotti E (2007) The role of CSA in the response to oxidative DNA damage in human cells. *Oncogene* **26**, 4336–4343.

Dörrie J, Gerauer H, Wachter Y, Zunino SJ (2001) Resveratrol induces extensive apoptosis by depolarizing mitochondrial membranes and activating caspase-9 in acute lymphoblastic leukemia cells. *Cancer Res.* **61**, 4731–4739.

Farber SA, Slack BE, Blusztajn JK (2000) Acceleration of phosphatidylcholine synthesis and breakdown by inhibitors of mitochondrial function in neuronal cells: a model of the membrane defect of Alzheimer's disease. *Faseb J.* **14**, 2198–2206.

Foresta M, Ropolo M, Degan P, Pettinati I, Kow YW, Damonte G, Poggi A, Frosina G (2010) Defective repair of 5-hydroxy-2′-deoxycytidine in Cockayne syndrome cells and its complementation by *Escherichia coli* formamidopyrimidine DNA glycosylase and endonuclease III. *Free Radic. Biol. Med.* **48**, 681–690.

Fortini P, Raspaglio G, Falchi M, Dogliotti E (1996) Analysis of DNA alkylation damage and repair in mammalian cells by the comet assay. *Mutagenesis* **11**, 169–175.

Frontini M, Proietti-De-Santis L (2009) Cockayne syndrome B protein (CSB): linking p53, HIF-1 and p300 to robustness, lifespan, cancer and cell fate decisions. *Cell Cycle* **8**, 693–696.

Iorio E, Mezzanzanica D, Alberti P, Spadaro F, Ramoni C, D'Ascenzo S, Millimaggi D, Pavan A, Dolo V, Canevari S, Podo F (2005) Alterations of choline phospholipid metabolism in ovarian tumor progression. *Cancer Res.* **65**, 9369–9376.

Kamenisch Y, Fousteri M, Knoch J, von Thaler AK, Fehrenbacher B, Kato H, Becker T, Dolle ME, Kuiper R, Majora M, Schaller M, van der Horst GT, van Steeg H, Rocken M, Rapaport D, Krutmann J, Mullenders LH, Berneburg M (2010) Proteins of nucleotide and base excision repair pathways interact in mitochondria to protect from loss of subcutaneous fat, a hallmark of aging. *J. Exp. Med.* **207**, 379–390.

Khobta A, Kitsera N, Speckmann B, Epe B (2009) 8-Oxoguanine DNA glycosylase (Ogg1) causes a transcriptional inactivation of damaged DNA in the absence of functional Cockayne syndrome B (Csb) protein. *DNA Repair (Amst.)* **8**, 309–317.

Kraemer KH, Patronas NJ, Schiffmann R, Brooks BP, Tamura D, DiGiovanna JJ (2007) Xeroderma pigmentosum, trichothiodystrophy and Cockayne syndrome: a complex genotype-phenotype relationship. *Neuroscience* **145**, 1388–1396.

Loupatty FJ, Clayton PT, Ruiter JP, Ofman R, Ijlst L, Brown GK, Thorburn DR, Harris RA, Duran M, Desousa C, Krywawych S, Heales SJ, Wanders RJ (2007) Mutations in the gene encoding 3-hydroxyisobutyryl-CoA hydrolase results in progressive infantile neurodegeneration. *Am. J. Hum. Genet.* **80**, 195–199.

Mancuso M, Orsucci D, Coppede F, Nesti C, Choub A, Siciliano G (2009) Diagnostic approach to mitochondrial disorders: the need for a reliable biomarker. *Curr. Mol. Med.* **9**, 1095–1107.

McKenna MJ, Medved I, Goodman CA, Brown MJ, Bjorksten AR, Murphy KT, Petersen AC, Sostaric S, Gong X (2006) N-acetylcysteine attenuates the decline in muscle Na+,K+-pump activity and delays fatigue during prolonged exercise in humans. *J. Physiol.* **576**, 279–288.

Muftuoglu M, de Souza-Pinto NC, Dogan A, Aamann M, Stevnsner T, Rybanska I, Kirkali G, Dizdaroglu M, Bohr VA (2009) Cockayne syndrome group B protein stimulates repair of formamidopyrimidines by NEIL1 DNA glycosylase. *J. Biol. Chem.* **284**, 9270–9279.

Myhre O, Andersen JM, Aarnes H, Fonnum F (2003) Evaluation of the probes 2′,7′-dichlorofluorescin diacetate, luminol, and lucigenin as indicators of reactive species formation. *Biochem. Pharmacol.* **65**, 1575–1582.

Newman JC, Bailey AD, Weiner AM (2006) Cockayne syndrome group B protein (CSB) plays a general role in chromatin maintenance and remodeling. *Proc. Natl. Acad. Sci. USA* **103**, 9613–9618.

Osenbroch PO, Auk-Emblem P, Halsne R, Strand J, Forstrom RJ, van der Pluijm I, Eide L (2009) Accumulation of mitochondrial DNA damage and bioenergetic dysfunction in CSB defective cells. *FEBS J.* **276**, 2811–2821.

Ott P, Clemmesen O, Larsen FS (2005) Cerebral metabolic disturbances in the brain during acute liver failure: from hyperammonemia to energy failure and proteolysis. *Neurochem. Int.* **47**, 13–18.

Page MM, Robb EL, Salway KD, Stuart JA (2010) Mitochondrial redox metabolism: aging, longevity and dietary effects. *Mech. Ageing Dev.* **131**, 242–252.

Pascucci B, D'Errico M, Parlanti E, Giovannini S, Dogliotti E (2011) Role of nucleotide excision repair proteins in oxidative DNA damage repair: an updating. *Biochemistry (Mosc.)* **76**, 4–15.

Qian W, Van Houten B (2010) Alterations in bioenergetics due to changes in mitochondrial DNA copy number. *Methods* **51**, 452–457.

Rezvani HR, Kim AL, Rossignol R, Ali N, Daly M, Mahfouf W, Bellance N, Taïeb A, de Verneuil H, Mazurier F, Bickers DR (2011) XPC silencing in normal human keratinocytes triggers metabolic alterations that drive the formation of squamous cell carcinomas. *J. Clin. Invest.* **121**, 195–211.

Ropolo M, Degan P, Foresta M, D'Errico M, Lasiglie D, Dogliotti E, Casartelli G, Zupo S, Poggi A, Frosina G (2007) Complementation of the oxidatively damaged DNA repair defect in Cockayne syndrome A and B cells by *Escherichia coli* formamidopyrimidine DNA glycosylase. *Free Radic. Biol. Med.* **42**, 1807–1817.

Rossignol R, Gilkerson R, Aggeler R, Yamagata K, Remington SJ, Capaldi RA (2004) Energy substrate modulates mitochondrial structure and oxidative capacity in cancer cells. *Cancer Res.* **64**, 985–993.

Sansbury BE, Jones SP, Riggs DW, Darley-Usmar VM, Hill BG (2011) Bioenergetic function in cardiovascular cells: the importance of the reserve capacity and its biological regulation. *Chem. Biol. Interact.* **191**, 288–295.

Tice RR, Agurell E, Anderson D, Burlinson B, Hartmann A, Kobayashi H, Miyamae Y, Rojas E, Ryu JC, Sasaki YF (2000) Single cell gel/comet assay: guidelines for in vitro and in vivo genetic toxicology testing. *Environ. Mol. Mutagen.* **35**, 206–221.

Tiziani S, Lodi A, Khanim FL, Viant MR, Bunce CM, Gunther UL (2009) Metabolomic profiling of drug responses in acute myeloid leukaemia cell lines. *PLoS ONE* **4**, e4251.

Tuo J, Jaruga P, Rodriguez H, Bohr VA, Dizdaroglu M (2003) Primary fibroblasts of Cockayne syndrome patients are defective in cellular repair of 8-hydroxyguanine and 8-hydroxyadenine resulting from oxidative stress. *Faseb J.* **17**, 668–674.

van der Pluijm I, Garinis GA, Brandt RM, Gorgels TG, Wijnhoven SW, Diderich KE, de Wit J, Mitchell JR, van Oostrom C, Beems R, Niedernhofer LJ, Velasco S, Friedberg EC, Tanaka K, van Steeg H, Hoeijmakers JH, van der Horst GT (2007) Impaired genome maintenance suppresses the growth hormone-insulin-like growth factor 1 axis in mice with Cockayne syndrome. *PLoS Biol.* **5**, e2.

Van Houten B, Woshner V, Santos JH (2006) Role of mitochondrial DNA in toxic responses to oxidative stress. *DNA Repair (Amst.)* **5**, 145–152.

Wieser W, Krumschnabel G (2001) Hierarchies of ATP-consuming processes: direct compared with indirect measurements, and comparative aspects. *Biochem J.* **355**, 389–395.

Wong HK, Muftuoglu M, Beck G, Imam SZ, Bohr VA, Wilson DM 3rd (2007) Cockayne syndrome B protein stimulates apurinic endonuclease 1 activity and protects against agents that introduce base excision repair intermediates. *Nucleic Acids Res.* **35**, 4103–4113.

Wu JJ, Quijano C, Chen E, Liu H, Cao L, Fergusson MM, Rovira II, Gutkind S, Daniels MP, Komatsu M, Finkel T (2009) Mitochondrial dysfunction and oxidative stress mediate the physiological impairment induced by the disruption of autophagy. *Aging (Albany NY)* **1**, 425–437.

Supporting Information

Additional supporting information may be found in the online version of this article:

Fig. S1 CS-A and CS-B primary fibroblasts present increased levels of intracellular ROS as detected by EPR.

Fig. S2 Mitochondrial function declines in CS-A and CS-B cells.

Fig. S3 CS-A and CS-B primary fibroblasts have decreased mitochondrial function.

Fig. S4 CS-A and CS-B cells display higher steady-state levels of ATP.

Fig. S5 CS-A and CS-B primary fibroblasts exposed to a ROS-inducing agent present increased levels of intracellular ROS and decreased mitochondrial membrane potential.

Fig. S6 CS-A and CS-B cells are hypersensitive to the killing effects of H_2O_2.

As a service to our authors and readers, this journal provides supporting information supplied by the authors. Such materials are peer-reviewed and may be re-organized for online delivery, but are not copy-edited or typeset. Technical support issues arising from supporting information (other than missing files) should be addressed to the authors.